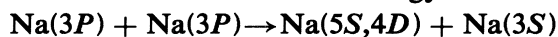


## Cross-section measurement for the energy-transfer collisions



M. Allegrini

*Istituto di Fisica Atomica e Molecolare del Consiglio Nazionale delle Ricerche,  
Via del Giardino, 3-56100 Pisa, Italy*

P. Bicchi

*Istituto di Fisica Atomica e Molecolare del Consiglio Nazionale delle Ricerche,  
Via del Giardino, 3-56100 Pisa, Italy  
and Istituto di Fisica dell'Università di Siena, Via Banchi di Sotto, 57-53100 Siena, Italy*

L. Moi

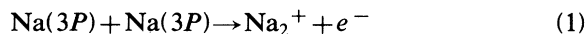
*Istituto di Fisica Atomica e Molecolare del Consiglio Nazionale delle Ricerche,  
Via del Giardino, 3-56100 Pisa, Italy*

(Received 15 September 1982)

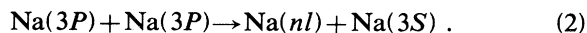
We report our measurements of the cross sections  $\sigma_{5S}$  and  $\sigma_{4D}$  for the electronic-energy-transfer process  $\text{Na}(3P) + \text{Na}(3P) \rightarrow \text{Na}(5S,4D) + \text{Na}(3S)$ . To obtain these cross sections we have measured the fluorescence intensity for the transitions  $5S \rightarrow 3P$ ,  $4D \rightarrow 3P$ , and  $3P \rightarrow 3S$  in sodium vapor excited with a cw dye laser. The study of this electronic energy transfer is complicated and there is a large disagreement ( $\gtrsim 10^4$ ) among reported measurements. We believe we have avoided most of the difficulties of previous experiments. Our results are  $\sigma_{5S} = (2.0 \pm 0.7) \times 10^{-15} \text{ cm}^2$  and  $\sigma_{4D} = (3.2 \pm 1.1) \times 10^{-15} \text{ cm}^2$ , and they are compared with the results of other experiments.

## I. INTRODUCTION

There is lively theoretical and experimental interest in understanding phenomena arising from resonance laser excitation in a dense vapor.<sup>1</sup> Most of the experiments concern sodium atoms excited to the  $3P$  level by pulsed or cw dye lasers over a wide range of atomic density. If the laser power density is less than  $10^2$ – $10^3 \text{ W cm}^{-2}$ , atomic multiphoton excitation and ionization can be neglected and the main mechanisms for production of ions and highly excited atoms are the associative ionization



and the energy-transfer collision process



There have been a number of experimental determinations of the rate constant for reaction (2), but there is a surprisingly large disagreement. As Table I reveals, the reported values differ by as much as a factor of  $10^5$ . We present here the results of a new determination which avoids a number of important source of systematic errors in previous experiments, and which we believe is reliable to 30%.

We believe that two sources of systematic errors contributed to the discrepancies between the previous measurements. First is the problem of accurately determining the effective volume of the laser-vapor interaction region. Second is the problem of controlling and measuring the density of excited  $\text{Na}(3P)$  atoms. We have largely overcome these problems with the use of a "capillary cell," a 7-cm long cylindrical cell of small (0.9 mm) radius connected to a sealed-off Na reservoir. The laser illuminates the entire volume of the cell through end windows of highly optical quality. The interaction volume is determined by the diameter of the cell and a carefully designed slit which accepts radiation only up to a distance of  $150 \mu\text{m}$  from the entrance window. These procedures assure that the interaction volume is accurately determined and that it is insensitive to variation in the optical-absorption length due to changes in the atom density or to laser intensity. The density of  $\text{Na}(3P)$  atom is determined by a novel calibration method which is discussed in detail below.

## II. APPROACH

The experiment involves continuously exciting Na to the  $3P$  state with a cw dye laser, and observing

TABLE I. Measured rate coefficients  $k_{nl}$  and derived collision cross section  $\sigma_{nl}$  for  $nl = 5S$  and  $4D$ .

Level	T (°C)	$k_{nl}$ (cm <sup>3</sup> sec <sup>-1</sup> ) <sup>a</sup>	$\sigma_{nl}$ (cm <sup>2</sup> ) <sup>a</sup>	Reference
4D	397	$1 \times 10^{-12}$	$9.0 \times 10^{-18}$ <sup>b</sup>	12
	227	$4.5 \times 10^{-15}$	$4.7 \times 10^{-20}$ <sup>b</sup>	11
	307 <sup>d</sup>		$\sim 10^{-14}$ <sup>c</sup>	14
	$\sim 324$	$2.46 \times 10^{-10} \pm 35\%$	$2.3 \times 10^{-15} \pm 35\%$	16
	210	$(3.0 \pm 0.9) \times 10^{-10}$	$(3.2 \pm 1.1) \times 10^{-15}$	this work
	277	$2.2 \times 10^{-11}$ <sup>b</sup>	$2.3 \times 10^{-16}$	13 theoretical
5S	227	$7.0 \times 10^{-15}$	$7.3 \times 10^{-20}$ <sup>b</sup>	11
	$\sim 324$	$1.63 \times 10^{-10} \pm 35\%$	$1.6 \times 10^{-15} \pm 35\%$	16
	210	$(1.9 \pm 0.6) \times 10^{-10}$	$(2.0 \pm 0.7) \times 10^{-15}$	this work

<sup>a</sup>Experimental errors are shown whenever they are given by the authors.

<sup>b</sup>Calculated from the relation  $k_{nl} = \sigma_{nl} \bar{v}$  with  $\bar{v} = (8kT/\pi\mu)^{1/2}$ .

<sup>c</sup>This value is derived from a measurement on the number of seed electrons produced via collisional ionization from the energy-pooling-populated  $4D$  state.

<sup>d</sup>The experiment used a weakly collimated effusive sodium beam. The oven temperature  $T = 307^\circ\text{C}$  corresponds to an average relative velocity of the atoms in the beam of  $\simeq 4 \times 10^4$  cm/sec.

the fluorescence from atoms in the  $3P$  state and also from the  $4D$  and  $5S$  states. From the ratio of these intensities the rate constants  $k_{nl}$  for reaction (2) are determined.

For our sodium densities the general evolution of the atomic system is governed by laser excitation, collisional transfer, and spontaneous emission. The rate equations are of the form

$$\dot{N}_{3P} = F - A(3P, 3S)N_{3P} - \sum_{n'l'} k_{n'l'} N_{3P}^2 + \sum_{n''l''} A(n''l'', 3P)N_{n''l''}, \quad (3)$$

$$\dot{N}_{nl} = k_{nl} N_{3P}^2 - \sum_{n'l'} A(nl, n'l')N_{nl} + \sum_{n''l''} A(n''l'', nl)N_{n''l''}, \quad (4)$$

where  $F$  is the number of atoms excited per second from the  $3S$  to the  $3P$  level and  $A(nl, n'l')$  is the spontaneous transition probability for  $|nl\rangle \rightarrow |n'l'\rangle$ . In Eq. (3) we have neglected stimulated emission because of the low laser power available in our experiment. However, we will not need to use this equation explicitly.

The rate constant  $k_{nl}$  for process (2) can be derived by solving Eq. (4) for  $N_{nl}$  in the steady-state condition. The general result is

$$k_{nl} = \frac{1}{N_{3P}^2} \left[ \sum_{n'l'} A(nl, n'l')N_{nl} - \sum_{n''l''} A(n''l'', nl)N_{n''l''} \right], \quad (5)$$

where the sum extends in principle to all levels allowed by the dipole selection rules. In practice, however, the equation can be considerably simplified. The energy pooling collisions are "pure" inelastic processes whose cross section rapidly vanishes as the energy defect  $\Delta E_{nl} = (2E_{3P} - E_{nl})$  increases beyond a few  $kT$ .

As shown in Fig. 1, the only levels which play important roles are  $5S$ ,  $4D$ , and  $4F$ . Unfortunately, the  $4F$ -level fluorescence is at  $1.8 \mu\text{m}$  and cannot be detected by our apparatus. However, evidence of the  $4F$  populating process is given by the fluorescence intensity of the  $3D \rightarrow 3P$  transition;<sup>2</sup> that is surprisingly high with respect to the large energy defect of the  $3D$  level ( $\Delta E_{3D} \simeq 12 kT$ ). This peculiarity can be justified assuming a cascade transition from the  $4F$  level.

Therefore we have restricted our analysis to the  $5S$  and  $4D$  states.

For these two levels we can neglect in Eq. (5) the second term representing the cascade radiation from the higher levels, without introducing appreciable error. Thus we can rewrite Eq. (5) as

$$k_{nl} = \frac{A(nl, 3P)N_{nl}}{N_{3P}^2} \left[ 1 + \sum_{n'l' \neq 3P} \frac{A(nl, n'l')}{A(nl, 3P)} \right], \quad (6)$$

where we emphasize the dominant term connecting the  $|nl\rangle$  and the  $|3P\rangle$  levels. The factor

$$\gamma_{nl} = \left[ 1 + \sum_{n'l' \neq 3P} \frac{A(nl, n'l')}{A(nl, 3P)} \right] \quad (7)$$

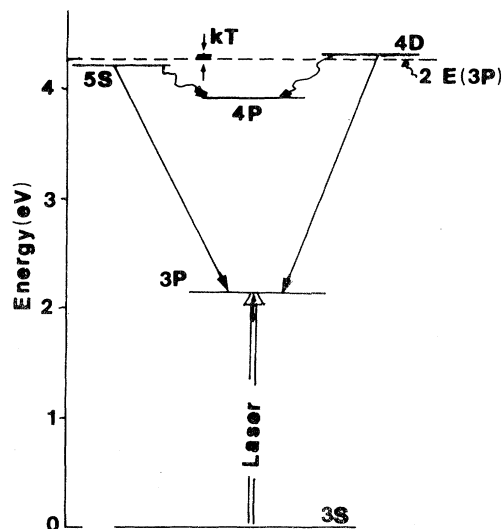


FIG. 1. Na energy-level diagram with the involved levels and transitions. The horizontal line represents the double of the 3P-level energy.

is a number expressing the branching ratio of the analyzed transition.<sup>3</sup> In our case each sum is reduced to a single term with the result  $\gamma_{4D} = 1.51$  and  $\gamma_{5S} = 1.74$ .

The measured quantities in our experiment are the intensities of the fluorescence lines. It is therefore convenient to use the relation between the transition probabilities and the line intensities (see, for example, Ref. 3) and to express  $k_{nl}$  as

$$k_{nl} = \alpha_{nl} \gamma_{nl} \frac{\omega_{3P \rightarrow 3S}}{\omega_{nl \rightarrow 3P}} \frac{I_{nl \rightarrow 3P}}{I_{3P \rightarrow 3S}} \frac{1}{N_{3P} \tau^*}, \quad (8)$$

where  $\alpha_{nl}$  is a factor which takes into account the instrumental response of the detecting apparatus and the calibration,  $I$  is the intensity of the detected transition, and  $\tau^*$  is the lifetime of the 3P level in the presence of the radiation trapping. Radiation trapping for the 4D, 5S  $\rightarrow$  3P transitions at our densities is negligible. From Eq. (8) it is clear that in order to determine  $k_{nl}$ , great care must be used in measuring  $N_{3P}$  and  $\tau^*$ .

To evaluate the  $N_{3P}$  density we make an absolute calibration of our apparatus by observing saturation fluorescence signals at fixed temperature but varying the intensity of the laser tuned to the  $3S_{1/2} \rightarrow 3P_{3/2}$  transition. To obtain the saturation of the fluorescence with the low-laser intensity available in our experiment, we need a relatively low atomic density. According to Cardinal and Measures,<sup>4</sup> at saturation the  $P_{3/2}$  and the ground-state  $S_{1/2}$  population densities are locked in the ratio of their degeneracies,<sup>5</sup> i.e.,

$$N_{3P_{3/2}} \simeq \frac{N_{at}}{1 + (g_{3S_{1/2}}/g_{3P_{3/2}})} = \frac{2}{3} N_{at}.$$

The behavior of the fluorescence intensity  $I_{3P \rightarrow 3S}$  versus the laser intensity  $I_L$  is complicated by the fact that the fluorescence intensity for an inhomogeneously broadened line varies as

$$\frac{I_L/I_S}{(1 + I_L/I_S)^{1/2}} = A(I_L), \quad (9)$$

whereas for a homogeneously broadened line it varies as

$$\frac{I_L/I_S}{1 + I_L/I_S} = B(I_L), \quad (10)$$

where  $I_S$  is the saturation parameter.<sup>6</sup> We use a multimode dye laser to excite the atoms. The mode spacing ( $\sim 290$  MHz) is small compared to the Doppler width ( $\sim 1$  GHz) and when the laser intensity is so high that the power broadening is comparable to or larger than the mode spacing this assures that the line is homogeneously broadened and that the power dependence is described by Eq. (10). At low power, however, one expects the power dependence to be given by Eq. (9).

Because the experimental results are very sensitive to the assumed power dependence of the line, we have carried out numerical studies of the fluorescence intensity over a wide range of parameters. The results could in all cases be accurately described by a linear combination of Eqs. (9) and (10) in the form

$$I_{3P \rightarrow 3S} = e^{-\xi I_L} A(I_L) + (1 - e^{-\xi I_L}) B(I_L), \quad (11)$$

where  $\xi$  is an adjustable parameter and  $A(I_L)$  and  $B(I_L)$  are independently normalized. Consequently, we have used this form to analyze our experiment, fitting the fluorescence line intensity to Eq. (11).

The evaluation of  $\tau^*$  will be described in Sec. IV.

### III. APPARATUS

A sketch of the experimental apparatus is shown in Fig. 2. The  $3P_{3/2}$  state is excited with a cw dye laser with a density power  $\leq 10 \text{ W cm}^{-2}$ . The bandwidth could be varied between 0.3 and 0.03 Å by using different intracavity etalons. The laser beam illuminates the principal axis of a cylindrical capillary cell whose internal radius is 0.9 mm. This cell is made in our laboratory utilizing as windows slices of glass rods flattened on the internal side and welded with the capillary tube. After welding, the ends of the cell also are optically flattened. A sidearm of the cell contains the sodium. Before loading, the cell is cleaned and baked for many hours on a vacu-

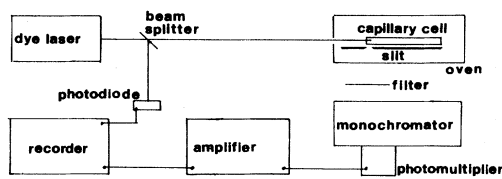


FIG. 2. Sketch of the experimental apparatus.

um system at a pressure of  $10^{-7}$  torr. No buffer gas is used. Because the cell is sealed and the vapor is saturated the atomic density  $N_{at}$  can be accurately determined from the temperature using the Nesmeyanov tables.<sup>7</sup>

The cell is placed in an oven in which a small temperature gradient is created in order to prevent window contamination. The temperature of the sodium reservoir is controlled to  $0.1^\circ\text{C}$  and it is varied between  $190^\circ\text{C}$  and  $210^\circ\text{C}$ , corresponding to an atomic density  $N_{at} \approx (1-6) \times 10^{12} \text{ cm}^{-3}$ . Close to the input window a narrow slit ( $\approx 150 \mu\text{m}$ ) is placed near to the cell to reduce the observation volume from which fluorescence is detected. The effective volume is  $4 \times 10^{-4} \text{ cm}^3$ .

The laser beam is focused to the diameter of the cell window so as to illuminate the whole cross section of the cell uniformly. To measure directly the laser intensity a beam splitter directs a small fraction of the laser beam into a photodiode. The fluorescence is analyzed at right angles by a 0.35-m monochromator and is detected by a photomultiplier with an S-20R cathode response.

To further minimize effects present in high vapor pressure, such as strong radiation trapping, collisional heating<sup>1,4</sup> of electrons produced by photoelectric effect in laser-wall interaction or by associative ionization, secondary collisional processes<sup>1</sup> etc., the experiment is performed at the lowest temperatures. Although this low atomic density decreases the intrinsic signal-to-noise ratio, this disadvantage is more than offset by the elimination of systematic errors which are the major problem in such experiments.

#### IV. EXPERIMENTAL PROCEDURE AND RESULTS

The experiment involves determining the rate constants  $k_{nl}$  using Eq. (8). The measured quantities are the principal fluorescence intensity  $I_{3P \rightarrow 3S}$ , the transfer fluorescence intensity  $I_{nl \rightarrow 3P}$ , and the excited-state density  $N_{3P}$ . The effective lifetime  $\tau^*$  is also required. Because the problem of radiation self-trapping is so complex and potentially troublesome,<sup>8</sup> we avoid measuring  $\tau^*$  directly. Instead we measure the product  $k_{nl}\tau^*$  which is equal to

$$\alpha_{nl}\gamma_{nl} \frac{\omega_{3P \rightarrow 3S}}{\omega_{nl \rightarrow 3P}} \frac{I_{nl \rightarrow 3P}}{I_{3P \rightarrow 3S}} \frac{1}{N_{3P}} \quad (12)$$

and from it determine  $k_{nl}$ , as described below.

The excited-state density  $N_{3P}$  is determined by observing the fluorescence at low temperature, where the line can be completely saturated and Eq. (11) can be mapped over its full range of variation. Typical results are shown in Fig. 3. The observed fluorescence intensity in all cases agrees with Eq. (11) within the experimental errors, namely, 5% or less. This operation is carried out before each determination of the rate constants.

Once the excited-state density is known at low temperature, the temperature is increased to the point where the fluorescence from the collisionally excited states becomes visible. At each temperature the line intensities  $I_{3P \rightarrow 3S}$  and  $I_{5S \rightarrow 3P}$ ,  $I_{4D \rightarrow 3P}$  are measured. To avoid operating the photomultiplier over a wide dynamic range, an optical attenuator is used to reduce the intense signal from the principal transition. The density at high temperature is found from the ratio of the accurately measured fluorescence intensity at high ( $T'$ ) and low ( $T^0$ ) temperature,

$$N_{3P}(T') = N_{3P}(T^0) \frac{I(T')}{I(T^0)} \frac{\tau^*}{\tau_0}, \quad (13)$$

where  $\tau^*$  is the trapped lifetime of the  $3P$  level at high temperature and  $\tau_0$  the natural lifetime at low temperature, and where the contribution of the  $P_{1/2}$  level to  $I(T')$  is taken into account. This method avoids the need to measure absolutely the system response efficiency  $\alpha_{nl}$  and requires only trivial corrections for such things as amplifier gain and possible nonlinearities.

We made a number of searches for fluorescence from higher-lying levels, but could not observe any

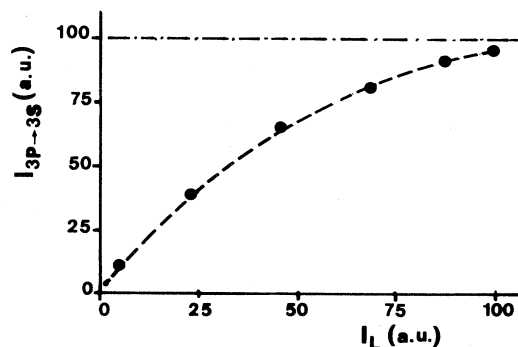


FIG. 3. Na  $3P$ - $3S$  fluorescence versus the laser intensity. The dashed curve represents the fit obtained by calculating the expression (11). The reported example was taken at  $T=150^\circ\text{C}$  and  $W_{L\text{max}} \approx 300 \text{ mW}$ . The errors are given by the size of the dots.

over our temperature range, validating the simplifying assumptions made in Eq. (8). At higher temperatures, however, contribution from high-lying states are easily observable.<sup>2</sup> Avoiding such contribution eliminates cascade transitions as a possible source of systematic errors.

Using these procedures the density  $N_{3P}$  was determined over a temperature range in which the atomic density varied by a factor  $\sim 6$ . Substitution of  $N_{3P}(T')$  in expression (12) provides the products  $k_{nl}\tau^{*2}/\tau_0$ . Results for  $k_{5S}\tau^{*2}/\tau_0$  are shown in Fig. 4. Over this small temperature range  $k_{5S}$  is expected to be constant because the relative energy of the colliding atoms remains constant to a few % as does the collisional frequency. Thus the temperature dependence is dominated by radiation trapping.

We have found that Milne's theory<sup>8</sup> of radiation trapping at low density is in good agreement with our data. We have solved the general equation of Milne for an optical depth  $d=0.35$  mm and have found values of  $\tau^*$  such that  $k_{5S}$  is essentially temperature independent. This is shown in Fig. 4, where  $\tau^{*2}/\tau_0$  versus temperature is reported on the right-hand side. The value  $d=0.35$  mm used in the calculation of the  $\tau^*$  is consistent with the geometrical configuration of our experiment considering that the major escape factor for the photons is through the entrance window. The fact that Milne's theory has been confirmed in the early experiment of Kibble *et al.*,<sup>9</sup> and the recent one of Garver *et al.*,<sup>10</sup> gives us further confidence in its validity under our conditions. Moreover, in Milne's theory at low temperature,  $\tau^*$  becomes the natural lifetime while high-temperature theories<sup>8</sup> often fail this simple test when applied to low-temperature data. Using this result we can extract the value for  $k_{nl}$  and results for  $k_{5S}$  are shown in Fig. 5. It is constant within experimental errors over the entire temperature range studied. The larger error at low temperature is due

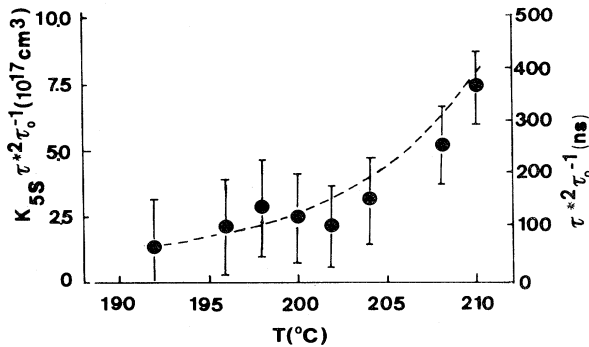


FIG. 4. Plot of  $k_{5S}(\tau^{*2}/\tau_0)$  values versus  $T$ . The dashed curve represents  $\tau^{*2}/\tau_0$  with  $\tau^*$  calculated from Milne's theory for an optical depth  $d=0.35$  mm.

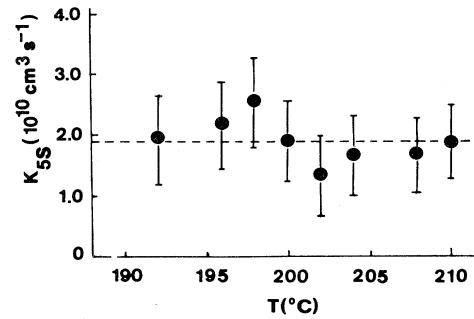


FIG. 5. Rate constant values versus  $T$  of the process (2) for the level 5S.

to the low counting rate. Similar results for  $k_{4D}$  are obtained. We estimate our measurements to be reliable within 30%.

Our results are (in  $\text{cm}^3/\text{sec}$ )

$$k_{5S} = (1.9 \pm 0.6) \times 10^{-10},$$

$$k_{4D} = (3.0 \pm 0.9) \times 10^{-10}.$$

The uncertainty, apart from statistical errors, is due to the determination of the ground-state density, to the self-trapping, to the calibration, and such things as laser fluctuations and system shift.

By applying the relation  $k_{nl} = \sigma_{nl} \bar{v}_{\text{rel}}$  with  $\bar{v}_{\text{rel}}$  the mean interatomic velocity

$$[\bar{v}_{\text{rel}} = (8kT/\pi\mu)^{1/2}],$$

we obtain (in  $\text{cm}^2$ )

$$\sigma_{5S} = (2.0 \pm 0.7) \times 10^{-15},$$

$$\sigma_{4D} = (3.2 \pm 1.1) \times 10^{-15}.$$

## V. DISCUSSION

Our results and the results of previous works are displayed in Table I. Disagreement between many of the measurements are marked. We believe that we have avoided many sources of errors which affected earlier measurements. In their experiment, Kushawaha and Leventhal<sup>11</sup> employed an open cell which can be a major source of error in determining the density. In such a case, the actual density can be much lower than calculated. The fact that molecular fluorescence could not be observed suggested that this may have been the case.

The experiment of Krebs and Schearer<sup>12</sup> operated at high temperature ( $T \approx 400^\circ\text{C}$ ) and used a buffer gas at high pressure ( $\sim 1$  atm), plus a powerful pulsed laser; all these conditions enhance the processes we have tried to avoid.

Our measurements are in good agreement with the theoretical value of Kowalczyk,<sup>13</sup> particularly

since his value is intended as a lower limit, having neglected curve crossing for internuclear separations  $\leq 15 \text{ \AA}$ .

The experiment of Le Gouët *et al.*<sup>14</sup>, which indirectly determines  $k_{nl}$ , confirms our values. This is particularly significant because it also supports other measurements<sup>15</sup> on the associative ionization process as in Eq. (1). The excellent agreement between our results and the recent measurements of Huennekens and Gallagher<sup>16</sup> lends added confidence.

#### ACKNOWLEDGMENTS

We are very grateful to Professor D. Kleppner for many helpful comments on the manuscript. Thanks are also due to Mr. M. Badalassi who prepared the "capillary" cells. One of us (M.A.) wishes to thank Professor A. Gallagher and Dr. J. Huennekens for many enlightening discussions.

<sup>1</sup>For a recent review, see T. B. Lucatorto and T. J. McIlrath, *Appl. Opt.* **19**, 3948 (1980); A. Kopystyńska and L. Moi, *Phys. Rep.* (in press).

<sup>2</sup>M. Allegrini, G. Alzetta, A. Kopystyńska, L. Moi, and G. Orriols, *Opt. Commun.* **19**, 96 (1976); **22**, 329 (1977).

<sup>3</sup>W. L. Wiese, M. W. Smith, and B. M. Miles, *Nat. Stand. Ref. Data Ser. Nat. Bur. Stand.* **22**, 4 (1969); E. M. Anderson and V. A. Zilitis, *Opt. Spektrosk.* **XVI**, 177 (1964) [*Opt. Spectrosc. (USSR)* **XVI**, 99 (1964)].

<sup>4</sup>R. M. Measures and P. G. Cardinal, *Phys. Rev. A* **23**, 804 (1981).

<sup>5</sup>At these densities the transfer from the  $3P_{3/2}$  to the  $3P_{1/2}$  level is negligible.

<sup>6</sup>See, e.g., A. Yariv, *Quantum Electronics* (Wiley, New York, 1975).

<sup>7</sup>A. N. Nesmeyanov, *Vapor Pressure of the Chemical Elements* (Elsevier, Amsterdam, 1963). Recent measurements of the atomic density (Ref. 16), carried out around 320°C, result in values larger than the 2–13 % of Nesmeyanov's.

<sup>8</sup>E. A. Milne, *J. London Math. Soc.* **1**, 40 (1926); T. Holstein, *Phys. Rev.* **72**, 1212 (1947); **83**, 1159 (1951); C. van Trigt, *ibid.* **181**, 97 (1969); *Phys. Rev. A* **1**, 1298

(1970); **4**, 1303 (1971); H. K. Holt, *ibid.* **13**, 1442 (1976).

<sup>9</sup>B. P. Kibble, G. Copley, and L. Krause, *Phys. Rev.* **153**, 9 (1967).

<sup>10</sup>W. P. Garver, M. R. Pierce, and J. J. Leventhal, *J. Chem. Phys.* **77**, 1201 (1982).

<sup>11</sup>V. S. Kushawaha and J. J. Leventhal, *Phys. Rev. A* **25**, 570 (1982); J. J. Leventhal, in *Photon Assisted Collisions and Related Topics*, edited by N. Rahman and C. Guidotti (Harwood Academic, Chur, 1982).

<sup>12</sup>D. J. Krebs and L. D. Scheerer, *J. Chem. Phys.* **75**, 3340 (1981).

<sup>13</sup>P. Kowalczyk, *Chem. Phys. Lett.* **68**, 203 (1979).

<sup>14</sup>J. L. Le Gouët, J. L. Picqué, F. Willeumier, J. M. Bizeau, P. Dhez, P. Kock, and D. L. Ederer, *Phys. Rev. Lett.* **48**, 600 (1982).

<sup>15</sup>V. S. Kushawaha and J. J. Leventhal, *Phys. Rev. A* **25**, 346 (1982).

<sup>16</sup>J. Huennekens and A. Gallagher, in *VIII International Conference on Atomic Physics, Göteborg, 1982, Program and Abstracts*, edited by I. Lindgren, A. Rosen, and S. Svanberg (Wallin and Dalholm, Lund, 1982), and *Phys. Rev. A* **27**, 771 (1983).